

RESEARCH ARTICLE

[View Article Online](#)
[View Journal](#)



Cite this: DOI: 10.1039/d5qi02493e

Lewis superacids for catalytic reductions of stronger element–oxygen double bonds with hydrosilanes

Daniel Franz, Thomas R. Frost, Sebastian Stigler and Shigeyoshi Inoue *

The main-group Lewis superacid complexes $(\text{pin}^F)_2\text{Si}\text{-MeCN}$ (**1** \cdot MeCN) and $(\text{pin}^F)_2\text{Ge}\text{-MeCN}$ (**2** \cdot MeCN) were successfully applied as promoters in the catalytic reduction of phosphine oxides (e.g., Me_3PO , Bu_3PO , and Ph_3PO), a sulfoxide (i.e., Me_2SO), and an amide (i.e., Me_2NCHO) to furnish the respective phosphines, dimethyl sulfide, and trimethylamine using silanes (e.g., PhSiH_3 and $(\text{EtO})_3\text{SiH}$) as hydrogen sources (pin^F = perfluoropinacolato). These substrates target difficult to reduce representatives of oxo compounds in comparison with, for example, the ketones or aldehydes often targeted in such types of catalytic reductions. As benchmark promoters, we also studied $\text{B}(\text{C}_6\text{F}_5)_3$ and HNTf_2 as reference (soft) Lewis superacid and Brønsted superacid, respectively ($\text{Tf} = \text{SO}_2\text{CF}_3$). Among the combinations of (pre) catalyst, substrate, and reducing agent investigated, the silicon complex **1** \cdot MeCN turned out to be the most versatile system, being the by far most potent (DMSO) or just slightly underperforming (R_3PO and DMF) promoter. Moreover, the hitherto undescribed Lewis acid base adducts **1** \cdot Me_2NCHO and **2** \cdot Me_2SO were synthesized, isolated, and structurally investigated using NMR spectroscopy and single-crystal XRD analysis.

Received 11th December 2025,
Accepted 10th January 2026

DOI: 10.1039/d5qi02493e
rsc.li/frontiers-inorganic

Introduction

In the wake of Stephan's groundbreaking report on catalytic dihydrogenation with frustrated Lewis pairs and Power's pioneering article on the resemblance of low valent main-group elements with transition metals, the study of s- and p-block complexes for homogeneous catalysis markedly intensified.¹ Stephan's, as well as Power's approaches, exploited the high reactivity profile of low-coordinate main group metal(lloid) atoms. Similarly, the pronounced Lewis acidity of silyl cations derives not only from their coulombic attraction but also from their low-coordinated state. Consequently, silyl cations have evolved after Lambert's seminal finding in 1993 into a vast field of catalytic applications.² As a more recent development, the use of strongly electron-withdrawing ligands was found to confer outstanding Lewis acidity to higher-coordinated and uncharged silicon complexes, as well, and the respective compounds were successfully applied in molecular catalysis.³ Notably, higher-coordinated cationic silicon complexes with outstanding Lewis acidity have also been reported.⁴

For the classification of Lewis acids, Krossing coined the term 'Lewis superacid' as a category of complexes with a larger

fluoride ion affinity (FIA) in the gas phase than antimony pentafluoride.⁵ Some controversy exists about the limitation of this threshold to a theoretical FIA, or whether experiment and theory need to coincide. More recently, Greb extended this concept to the definition of 'soft Lewis superacids', that is, molecular Lewis acids that have a larger hydride ion affinity (HIA) than $\text{B}(\text{C}_6\text{F}_5)_3$ in the gas phase.^{3b} Perhalogenated species of the chelate fashioned catecholato ligand and its derivatives have been established as particularly suitable ligands for various Si and Ge complexes that meet the criteria for Lewis superacidity (selected species A–C, Fig. 1).⁶ In 2021, we reported the silicon complex **1** \cdot MeCN, which bears the bidentate and strongly electron-withdrawing perfluoropinacolato ligand and abstracts fluoride from AgSbF_6 in acetonitrile solution (Fig. 1).⁷ Also, the heavier germanium congener **2** \cdot MeCN was described, which exhibited larger FIA and HIA values (Fig. 1).⁸ These compounds promoted catalytic conversions such as hydrodefluorination and hydrosilylation (i.e., reduction) of double bonds, as well as polyether degradation.^{7–9} In a detailed fashion we had investigated the catalytic hydrosilylation (i.e., reduction) of ketones and aldehydes with **1** \cdot MeCN.⁷ In this work, we focus on more difficult to reduce element oxygen double bonds as found in phosphine oxides, sulfoxides, and amides using **1** \cdot MeCN and **2** \cdot MeCN as promoters. Moreover, we compare the catalytic activities of these with the ubiquitous benchmark Lewis acid $\text{B}(\text{C}_6\text{F}_5)_3$ and the strong Brønsted acid HNTf_2 ($\text{Tf} = \text{SO}_2\text{CF}_3$).

TUM School of Natural Sciences, Department of Chemistry, Catalysis Research Center and Institute of Silicon Chemistry, Technical University of Munich, Garching bei München, Germany. E-mail: s.inoue@tum.de



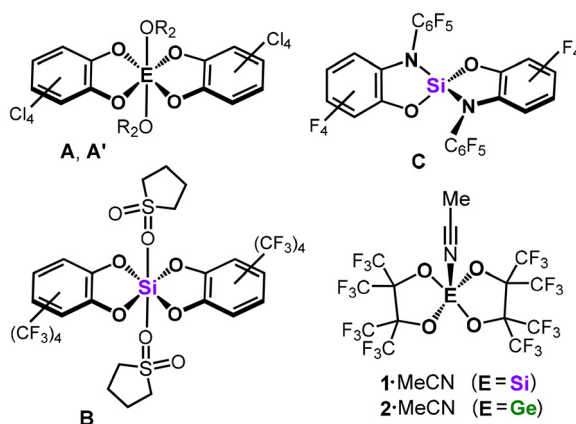


Fig. 1 Selected group 14 Lewis acids. The biscatecholato complexes **A**, **A'**, and **B**, as well as the bis(ortho-amidophenolato) compound **C** and the bis(perfluoropinacolato) complexes **1**·MeCN and **2**·MeCN (**A**: E = Si, R = Et; **A'**: E = Ge, R = H).

Results and discussion

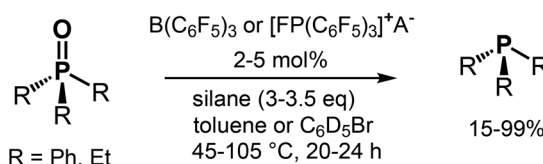
Phosphine oxide reductions

Phosphines are used in many synthetic applications because the formation of the strong phosphorus–oxygen double bond often drives a reaction, as seen in the Wittig and Mitsunobu reactions.¹⁰ The reduction of phosphine oxides back to the corresponding phosphines is attractive in the light of waste material recycling. Catalytic amounts of titanium(IV) alkoxy compounds were reported by Lawrence to catalyze the reduction of tertiary phosphine oxides by silanes.¹¹ Beller used copper halides and copper(II) triflate to facilitate the reduction of secondary and tertiary phosphine oxides with organosilanes.¹² Notably, non-catalytic methods for the reduction of tertiary phosphine oxides using highly reactive silanes (*e.g.*, PhSiH₃, Cl₃SiH, and Si₂Cl₆) were reported about 60 years ago and commonly required harsh reaction conditions.¹³ Other procedures that work without a catalyst typically implement hydroboranes or aluminum hydrides and the reader is referred to the respective reviews for details.¹⁴ Prominent examples for phosphine oxide reduction by main-group promoters rely on potent Lewis acids of boron (*e.g.*, B(C₆F₅)₃, (2-Cl-C₆H₄)₂BOH) or highly Lewis acidic phosphonium cations (Fig. 2, rows 1 and 2).¹⁵ More recently, Greb described the implementation of the silicon Lewis superacid **B** in the reduction of Et₃PO and Ph₃PO at 100 °C in toluene using 3 eq. of PhSiH₃ as a reducing agent (Fig. 2, row 3).^{6c}

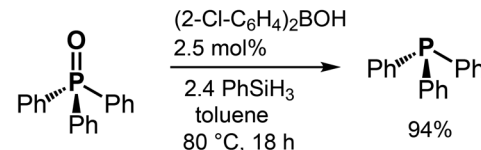
Notably, the experimental assessment of Lewis acidity is commonly conducted by the use of phosphine oxides and ³¹P NMR analysis, that is, the Gutmann–Beckett method.¹⁶ Accordingly, many Lewis superacids have been probed for complexation of Et₃PO, but the further conversion of these complexes, if formed, has often not been investigated.

In the light of Greb's result, we set out to probe the catalytic activity of **1**·MeCN and **2**·MeCN for phosphine oxide reduction using Bu₃PO, Me₃PO, and Ph₃PO as substrates. The ubiquitous

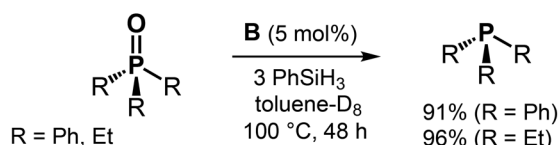
Oestreich & Stephan 2016



Blanchet 2017



Greb 2021



This work

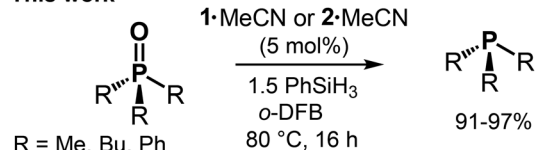


Fig. 2 Selected catalytic tertiary phosphine oxide reductions to phosphine using main group complexes ($A^- = B(C_6F_5)_4^-$; silane = PhSiH₃, (EtO)₃SiH; *o*-DFB = *ortho*-difluorobenzene).

Et₃PO was left out due to its higher pricing and lower convenience (*i.e.*, waxy nature of the solid) which renders it less suitable for large-scale applications. As expected, the use of PhSiH₃ resulted in the production of phosphine and the results of our catalytic conversions are shown in Table 1. The conversion of Bu₃PO with 1.5 eq. of PhSiH₃ and **1**·MeCN or **2**·MeCN as a promoter (5 mol%) furnished the respective phosphine in a near-quantitative fashion (97% or 96%) after 16 h in *ortho*-difluorobenzene (*o*-DFB) at 80 °C (Table 1, entries 1 and 2). Decreasing the catalyst load to 1 mol% **2**·MeCN resulted in a markedly lower yield (75%), which might possibly be compensated by a longer reaction time (Table 1, entry 3). The alternative reducing agents Et₃SiH (5.5 eq.) and pinacolborane (HBpin, 4.5 eq.) were also tested and resulted in practically no formation of phosphine (Et₃SiH) and high phosphine yield (HBpin, 89%), respectively, which agrees with the expected deoxyhydrogenation activity of these compounds (Table 1, entries 4 and 5). In the context of applying the germanium complex **2**·MeCN, we had described its reaction to a germylene species of the type pin^FGe (pin^F = ((CF₃)₂CO)₂) upon reaction with Et₃SiH.⁸ Though this reactivity is mostly favored in the absence of electron-pair donors, it may gain relevance at elevated temperature and in the presence of excess hydrosilane. Thus, we tested the germylene adduct (pin^FGe)₂·(1,4-dioxane) ((3)₂·diox) as a promoter in catalytic phosphine oxide



Table 1 Catalytic reduction of phosphine oxides to phosphines

R ₃ PO R = Me, nBu, Ph	catalyst (mol%) reductant o-DFB, T, 16 h	R ₃ P + siloxanes			
		Red. (eq.)	T [°C]	Yield ^a [%]	
		R	Cat. (mol%)		
1	nBu	1-MeCN (5)	PhSiH ₃ (1.5)	80	97
2	nBu	2-MeCN (5)	PhSiH ₃ (1.5)	80	96
3	nBu	2-MeCN (1)	PhSiH ₃ (1.5)	80	75
4	nBu	2-MeCN (5)	Et ₃ SiH (5.5)	110	<1
5	nBu	2-MeCN (5)	HBpin (4.5)	80	89
6	nBu	(3) ₂ -diox (2.5)	PhSiH ₃ (1.5)	80	52
7	nBu	(3) ₂ -diox (2.5)	Et ₃ SiH (5)	120	<1
8	nBu	HNTf ₂ (5)	PhSiH ₃ (1.5)	80	99
9	nBu	None	PhSiH ₃ (1.5)	80	20
10	Me	1-MeCN (5)	PhSiH ₃ (1.5)	80	91 ^b
11	Ph	2-MeCN (5)	PhSiH ₃ (1.5)	80	69

(3)₂-diox = (pin^FGe)₂·(1,4-dioxane), pin^F = perfluoropinacolato. ^a Yield determined using ³¹P{¹H} NMR by the addition of tris(2,4-di-*tert*-butylphenyl) phosphite as an internal standard (after the conversion).

^b Yield determined using ¹H NMR by the addition of 4,4'-di-*tert*-butylbiphenyl as an internal standard (at conversion start).

reduction, as well, after we had synthesized it independently as described in the literature.⁸ In fact, the use of (3)₂-diox (5 mol% loading in Ge) afforded markedly lower yield (52%) of Bu₃P in combination with PhSiH₃ (1.5 eq.) in comparison with the reactions with 1-MeCN and 2-MeCN (Table 1, entries 6, 7, cf. entries 1 and 2). We assume that the reduced Lewis acidity of the germylene, as compared to the germane, accounts for the decreased activity of the former. Accordingly, the partial conversion of 2-donor into 3-donor might hamper the catalytic performance of 2-MeCN in the course of the reaction and come into effect for longer reaction times or lower catalyst loadings, as we had observed (Table 1, entry 3). For comparing our Lewis acids with a strong Brønsted acid, we used HN (SO₂CF₃)₂ as a (pre)catalyst, and the reduction of Bu₃PO proceeded similarly to that of our Si and Ge promoters (Table 1, entry 8). One must note that in the absence of any promoter, the phosphine oxide was also reduced to a non-negligible degree (20%, Table 1, entry 9), which agrees with the literature reports.¹⁷ We also probed Me₃PO as the substrate to find complete consumption of the oxide and formation of Me₃P (91%, the non-quantitative detected yield is attributed to partial loss of volatile Me₃P to the headspace) after just 5 h at 80 °C and, thus, considerably shorter than the *ca.* 16 h required for the reduction of the bulkier Bu₃PO under very similar conditions (Table 1, entry 10 vs. 1). In stark contrast, Ph₃PO was more difficult to reduce as we found only 69% of the respective phosphine after the full 16 h of reaction period (Table 1, entry 11). For comparison, Oestreich and Stephan reported near-quantitative conversion of Ph₃PO with the use of B(C₆F₅)₃ (5 mol%) in toluene at 105 °C over 20 h.^{15a}

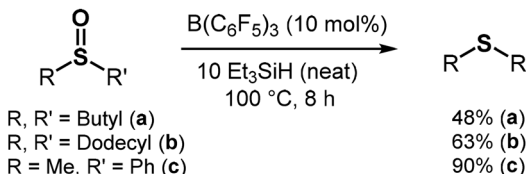
Dimethylsulfoxide reductions

With our successful reduction of the P=O double bond as a starting point, we set out to apply similar conditions to the

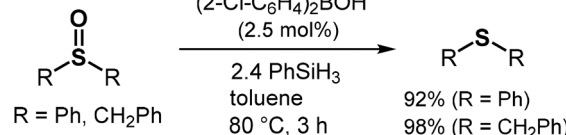
reduction of S=O double bonds. Me₂SO (DMSO) marks one of the most widespread sulfoxides due to its application as a polar-aprotic solvent. Generally, sulfur possesses a higher electronegativity and a smaller atomic radius in comparison with phosphorus. These attributes will affect bond polarization and π -interaction with oxygen and, in consequence, grant a lesser degree of zwitterionic character to the S=O double bond as compared to the P=O double bond. The generally higher electron affinity of sulfur over phosphorus should facilitate the reduction of formal oxidation state S(+IV) to S(+II) as compared to the reduction of P(+V) to P(+III). The conversion of sulfoxides to sulfides is a vast field employing transition metal catalysis,¹⁸ main group catalysis,^{15b,19} electrochemical procedures,²⁰ photochemical,²¹ and catalyst-free methods (Fig. 3).²² DMSO is one of the most fundamental sulfoxides and, due to its occurrence in the biosphere, the DMSO/DMS redox system plays an important role in biochemistry, as well as environmental and food analytics. For example, reductions include the use of molybdenum-containing enzyme DMSO reductase²³ or rhodium(III) and molecular hydrogen.²⁴ Trace analysis of DMSO in natural water after its reduction to DMS with NaBH₄ has been described.²⁵ The occurrence of DMS in beer brewing processes is notable, as well.²⁶

We converted DMSO with PhSiH₃ (1.5 eq.) under the addition of 1-MeCN as a catalyst (5 mol%) in C₆D₆ at room temperature (RT). As a result, we observed full consumption of

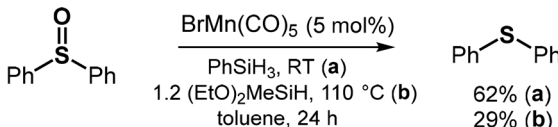
Oestreich 2017



Blanchet 2017



Fernandes 2024



This work (selection)

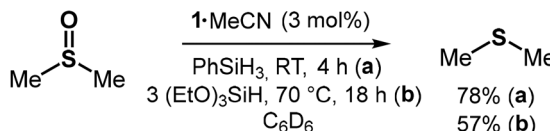


Fig. 3 Selected catalytic reductions of sulfoxides to sulfides using hydrosilane reducing agents (RT = room temperature).



the DMSO and major conversion to Me_2S (DMS, 73%) within 2 hours (using ^1H and ^{13}C NMR analysis with 4,4'-di-*tert*-butyl-biphenyl as the internal standard, Table 2, entry 1). This contrasts the increased temperature (80 °C) and longer reaction time (5 h) required for the reduction of Me_3PO with PhSiH_3 . The discrepancy between the converted DMSO (>99%) and the determined DMS yield (73%) we attribute to a larger relevance of side-reactions for the conversion of this substrate as compared to the phosphine oxide reductions. As expected, decreasing the load of **1**·MeCN and the equivalents of PhSiH_3 resulted in lower conversion rates (Table 2, entries 2, 3 and 4). For the phosphine oxide reduction, the use of **2**·MeCN as a (pre)catalyst had afforded just marginally less efficient conversions of the substrates. Remarkably, the catalytic DMSO reduction with PhSiH_3 showed a substantially diminished performance at RT when using this germanium complex as a promoter (Table 2, entries 5 and 6). Using catalytic amounts of the preformed DMSO complex **2**·Me₂SO (see the supplementary information for its isolation) instead of **2**·MeCN had a negligible effect on the conversion rate (Table 2, entry 7). It is reasonable to assume that a 'softer' sulfur atom has a higher affinity to the Ge center in **2** as it has to the 'harder' Si center in **1**. Thus,

2·MeCN will suffer more strongly from 'catalyst poisoning' by the sterically unhindered product Me_2S . We also employed both the reference acids $\text{B}(\text{C}_6\text{F}_5)_3$ and HNTf_2 as (pre)catalysts, which in resemblance to **2**·MeCN, turned out to perform substantially worse than the silicon Lewis acid **1**·MeCN (Table 2, entries 8 and 9). Notably, when no promoter was applied, 14% DMSO was consumed to yield 8% DMS at 100 °C over 24 h (Table 2, entry 10). Moreover, we investigated the use of Et_3SiH and $(\text{EtO})_3\text{SiH}$ as alternative reducing agents. These are less atom economical but commonly cheaper and more suitable for process upscaling than PhSiH_3 . The Et_3SiH reducing agent (4 eq.) proved ineffective in our hands: very harsh conditions (100 °C, 24 h) provided only 6% yield in DMS (28% conversion of DMSO) when applying the potent **1**·MeCN as a (pre)catalyst (Table 2, entry 11). In contrast, $(\text{EtO})_3\text{SiH}$ (4 eq.) afforded conversion to DMS in a moderate yield (52%) at RT in C_6D_6 using **1**·MeCN (5 mol%), though on a notably longer timescale (72 h, Table 2, entry 12). Changing the solvent (C_6D_6 for CDCl_3) and lowering the equivalents of hydrides had only a minor impact on the reaction outcome (Table 2, entry 13). Conducting the catalysis at 70 °C in C_6D_6 boosted the conversion rate with only a negligible impact on product distribution (Table 2, entry 14). In resemblance to our finding with PhSiH_3 , three equivalents of hydride were required for an effective reduction: the use of only 2 eq. $(\text{EtO})_3\text{SiH}$ resulted in incomplete DMSO conversion (70%) to afford 39% DMS at 70 °C (3 mol% load with **1**·MeCN) even at prolonged reaction times (Table 2, entry 15). The high performance of **1**·MeCN as a promoter was verified by decreasing the load down to 1 mol%, which delivered almost 2/3 of the DMS yield after the same reaction time as with 5 mol% load (Table 2, entry 16 vs. entry 12). With $(\text{EtO})_3\text{SiH}$ as a reducing agent, the use of germanium complex **2**·MeCN as a (pre)catalyst was, yet again, less effective than using the silicon Lewis acid (Table 2, entries 17 and 18). The Brønsted superacid promoter $\text{HN}(\text{Tf})_2$ was also markedly less effective than **1**·MeCN (Table 2, entries 19 and 20). Notably, we observed the separation of oil and solid from the reaction solution. We found the combination of $(\text{EtO})_3\text{SiH}$ with $\text{B}(\text{C}_6\text{F}_5)_3$ as a (pre)catalyst least suitable: with a load of 5 mol% and use of 4 eq. silane we could not observe DMS formation even after allowing the experiment to run a couple of days beyond the 72 h time mark (Table 2, entry 21). The outcome that the boron Lewis acid does not promote the DMSO reduction in combination with $(\text{EtO})_3\text{SiH}$ (at RT) but performs moderately when brought together with PhSiH_3 needs to be considered in the light of the respective ^{11}B NMR data: the ^{11}B NMR spectrum of the triethoxysilane conversion reveals a singlet at -0.4 ppm ($h_{1/2} = 230$ Hz), which we ascribe to $[\text{EtOB}(\text{C}_6\text{F}_5)_3]^-$, though $\text{Me}_2\text{SB}(\text{C}_6\text{F}_5)_3$ is a conceivable species, as well.²⁷ The ^{11}B analysis of the PhSiH_3 reaction similarly shows a major singlet at -0.2 ppm ($h_{1/2} = 240$ Hz) but also reveals a doublet at -24.7 ppm ($J = 80$ Hz) of minor intensity (see Fig. S21). The doublet can be assigned to the $[\text{HB}(\text{C}_6\text{F}_5)_3]^-$ anion, which was reported for catalytic conversions using combinations of hydrosilane and tris(pentafluorophenyl)borane and, of course, for catalytic dihydrogenations with frustrated Lewis pairs con-

Table 2 Catalytic reduction of DMSO to DMS using silanes

Me ₂ SO	catalyst (mol%)		Me ₂ S + siloxanes		
	silane	C ₆ D ₆ , T, t			
Cat. (mol%)	Silane (eq.)	T	t	Yield ^a [%]	
1	1 ·MeCN (5)	PhSiH ₃ (1.5)	RT	2 h	73
2	1 ·MeCN (3)	PhSiH ₃ (1)	RT	4 h	78 ^b
3	1 ·MeCN (1)	PhSiH ₃ (1)	RT	4 h	53 ^b
4	1 ·MeCN (3)	PhSiH ₃ (2/3)	RT	24 h	66 ^c
5	2 ·MeCN (5)	PhSiH ₃ (1.5)	RT	3 h	9
6	2 ·MeCN (3)	PhSiH ₃ (1)	RT	4 h	6
7	2 ·DMSO (3)	PhSiH ₃ (1)	RT	4 h	12 ^d
8	$\text{B}(\text{C}_6\text{F}_5)_3$ (5)	PhSiH ₃ (1)	RT	18 h	13
9	HNTf_2 (5)	PhSiH ₃ (1.5)	RT	2 h	12 ^e
10	None	PhSiH ₃ (3)	100 °C	24 h	8
11	1 ·MeCN (5)	Et_3SiH (4)	100 °C	24 h	6
12	1 ·MeCN (5)	$(\text{EtO})_3\text{SiH}$ (4)	RT	72 h	52 ^f
13	1 ·MeCN (5)	$(\text{EtO})_3\text{SiH}$ (3)	RT	72 h	40 ^g
14	1 ·MeCN (3)	$(\text{EtO})_3\text{SiH}$ (3)	70 °C	18 h	57
15	1 ·MeCN (3)	$(\text{EtO})_3\text{SiH}$ (2)	70 °C	36 h	39 ^h
16	1 ·MeCN (1)	$(\text{EtO})_3\text{SiH}$ (4)	RT	72 h	31
17	2 ·MeCN (5)	$(\text{EtO})_3\text{SiH}$ (4)	RT	72 h	26
18	2 ·MeCN (3)	$(\text{EtO})_3\text{SiH}$ (3)	70 °C	18 h	12
19	HNTf_2 (5)	$(\text{EtO})_3\text{SiH}$ (4)	RT	72 h	10 ^e
20	HNTf_2 (5)	$(\text{EtO})_3\text{SiH}$ (3)	RT	72 h	11 ⁱ
21	$\text{B}(\text{C}_6\text{F}_5)_3$ (5)	$(\text{EtO})_3\text{SiH}$ (4)	RT	72 h	<1
22	None	$(\text{EtO})_3\text{SiH}$ (5)	100 °C	24 h	<1

^a Yield of DMS was determined by addition of 1,4-di-*tert*-butyl-biphenyl as internal standard. ^b DMSO was fully consumed and yield was increased after 12 h. ^c Monitoring for additional 6 h resulted only in negligible change. ^d DMSO was fully consumed and 78% yield achieved after 13 h at 70 °C. ^e An oil separated from the mixture. ^f After a total of 96 h, DMSO was fully consumed and 58% yield was achieved. ^g CDCl_3 was used as the solvent instead of C_6D_6 . ^h No further conversion by additional heating for 12 h. ⁱ CDCl_3 was used as the solvent and a solid separated after few hours.



taining this borane Lewis acid.²⁸ The borohydride anion may indicate the formation of highly Lewis acidic silyl cation or the borohydride itself may act as a hydride transfer reagent. Finally, it is of note that without the application of a catalyst, no relevant consumption of DMSO was indicated by the ¹H NMR analysis at 100 °C for 24 h using 5 eq. of (EtO)₃SiH (Table 2, entry 22).

Dimethylformamide reductions

DMF is difficult to reduce due to the delocalization of the nitrogen lone pair into the amide system, which renders the carbonyl carbon atom less electrophilic. It is used in large quantities as a solvent in the synthesis of peptides.²⁹ DMF has a high boiling point (153 °C) and is commonly known for its hepatotoxicity.³⁰ This combination of properties makes complete removal of the solvent from products most desirable, yet difficult. The ability to reduce DMF to volatile trimethylamine (boiling point 3 °C) would be beneficial for clean-up of reactions where large quantities of DMF waste are produced. Several methods for the catalytic reduction of DMF to Me₃N by hydrosilanes using transition metal compounds as promoters have been described.³¹ Cui has reported the use of Cs₂CO₃ as a suitable catalyst for the reduction of DMF (and other amides) using phenylsilanes (Fig. 4).³²

Given the potency of the Lewis acids **1**·MeCN and **2**·MeCN in the catalytic reduction of R₃PO and Me₂SO with silanes, we tested these systems for the transformation of DMF to Me₃N using PhSiH₃, as well. Promoting the reaction with **1**·MeCN (5 mol%) in toluene-D₈ furnished trimethylamine in a near-quantitative fashion (99%) at 110 °C over 12 h (Table 3, entry 1). Under milder reaction conditions (80 °C), a smaller ratio of

Me₃N was detected (71%) even after longer processing (24 h), which underlines the stability of this amide bond (Table 3, entry 2). The Ge complex **2**·MeCN exhibited decreased catalytic activity (61%, Table 3, entry 3). The benchmark soft lewis superacid B(C₆F₅)₃ performed similarly to **1**·MeCN after 22 h (Table 3, entry 4). The ¹¹B NMR spectra of the process revealed a signal at -24.7 ppm, which can be assigned to HB(C₆F₅)₃, and this observation resembles the DMSO reduction with B(C₆F₅)₃ and PhSiH₃ described above. In the absence of a Lewis acid catalyst, no conversion of DMF was observed in toluene after 48 hours at 110 °C using 1.5 equivalents of PhSiH₃ (Table 3, entry 5). To our knowledge, this is the first report of an uncharged tetrel Lewis superacid to successfully catalyze the reduction of an amide to an amine.

Synthesis and isolation of **1**·Me₂NCHO and **2**·Me₂SO

In order to independently synthesize possible intermediates of our catalytic conversions, we reacted **1**·MeCN and **2**·MeCN with 1.3 eq. of DMF and DMSO, respectively (Scheme 1). The analytically pure Lewis acid base complexes **1**·Me₂NCHO and **2**·Me₂SO were isolated in good yields (89% and 84%) and characterized by NMR spectroscopy, combustion analysis (CHNS), mass spectrometry, and single-crystal XRD (SC-XRD) study.

As a notable characteristic in the ¹H NMR spectrum of **1**·Me₂NCHO the signals of the Si-coordinated DMF are notably shifted to lower fields (δ = 8.32, 3.33, and 3.18 ppm) as compared to “free” DMF in CD₃CN.³³ Suitable crystals of **1**·Me₂NCHO for SC-XRD analysis were obtained from a saturated CH₂Cl₂/MeCN (2 : 1) solution at -35 °C. The study reveals a silicon center that is coordinated in a trigonal bipyramidal fashion with the DMF ligand assuming an equatorial position (Fig. 5, top). The C=O bond length in **1**·Me₂NCHO amounts to C1–O1 = 1.296(4) Å, which is elongated as compared to DMF in the solid state (note: crystalline DMF forms a hydrogen bonding network with a mean C–O of 1.23 Å).³⁴ This suggests a weakening in the C=O bond and may facilitate the hydride-induced reductive cleavage.

Cui 2013, 2018

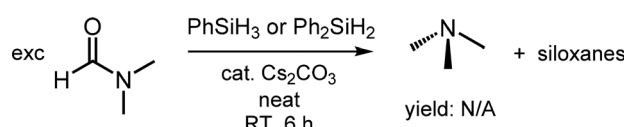
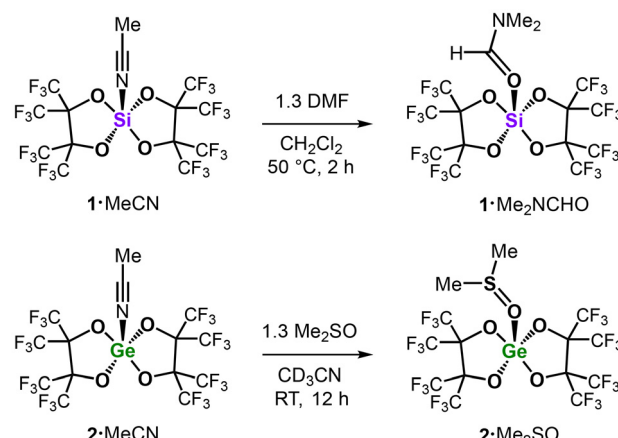


Fig. 4 Reduction of DMF to Me₃N as described by Cui.

Table 3 Catalytic reduction of DMF to Me₃N using silanes

Me ₂ NCHO	catalyst (mol%)	Me ₃ N + siloxanes
	1.5 PhSiH ₃ C ₆ D ₆ , T, t	
Cat. (mol%)	Solvent	T [°C]
1	1 ·MeCN (5)	C ₇ D ₈
2	1 ·MeCN (5)	C ₆ D ₆
3	2 ·MeCN (5)	C ₆ D ₆
4	B(C ₆ F ₅) ₃ (5)	C ₆ D ₆
5	None	<i>o</i> -DFB
		t
		Yield ^a [%]
1		110
2		80
3		80
4		80
5		110
		12 h
1		12 h
2		24 h
3		24 h
4		22 h
5		48 h
		99
2		71
3		61
4		70 ^b
5		0

^a Yield determined using ¹H NMR with 4,4-di-*tert*-butyl-biphenyl as an internal standard. ^b Near-quantitative consumption of DMF.



Scheme 1 Synthesis of the tetrel complexes **1**·Me₂CH and **2**·Me₂SO.



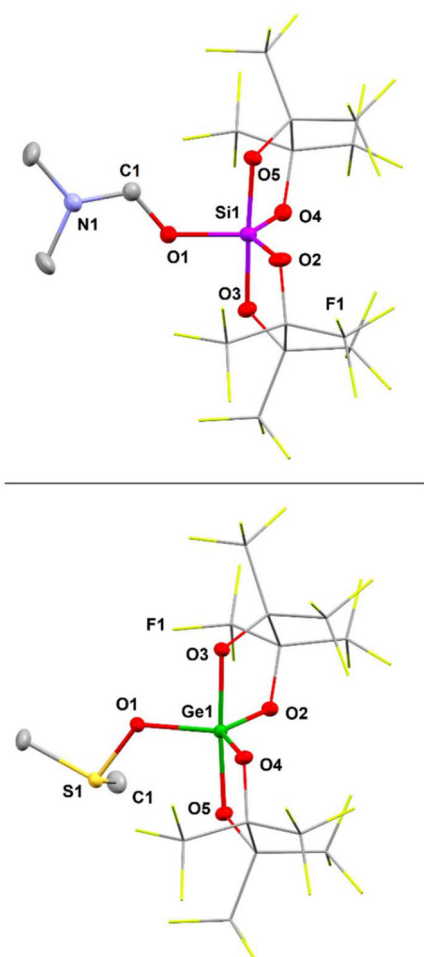


Fig. 5 Molecular structure of **1**–Me₂NCHO (top) and **2**–Me₂SO (bottom) as ellipsoid plots (50% probability level) as derived from SC-XRD study. Hydrogen atoms are omitted for clarity. The (C(CF₃)₂)₂ groups are displayed as capped sticks. One lattice MeCN is not shown (bottom). Selected structural parameters [Å, °]: Top: Si1–O1 = 1.718(2), Si1–O2 = 1.686(2), Si1–O3 = 1.743(2), Si1–O4 = 1.685(2), Si1–O5 = 1.730(2), C1–N1 = 1.289(5), C1–O1 = 1.296(4); O1–Si1–O2 = 117.9(1), O1–Si1–O4 = 112.9(1), O2–Si1–O4 = 129.1(1). Bottom: Ge1–O1 = 1.820(1), Ge1–O2 = 1.801(1), Ge1–O3 = 1.836(1), Ge1–O4 = 1.802(1), Ge1–O5 = 1.854(1), S1–O1 = 1.596(1), O1–Ge1–O2 = 113.5(1), O1–Ge1–O4 = 118.6(1), O2–Ge1–O4 = 127.9(1).

In the ¹H NMR spectrum of **2**–Me₂SO, the singlet for the CH₃ groups of coordinated DMSO at 3.10 ppm ($J_{\text{H}^{13}\text{C}} = 144$ Hz) is notable, which is markedly shifted to lower field as compared to the value for “free” Me₂SO in CD₃CN (2.50 ppm).³³

Crystals of **2**–Me₂SO, suitable for SC-XRD analysis, were crystallized directly from the reaction mixture at –25 °C and the molecular structure of **2**–Me₂SO in the solid state marks a trigonal bipyramidal coordinate Ge center (sum of the equatorial bond angles ≈ 360°, Fig. 5, bottom). The bond to the oxygen atom of the (equatorial) DMSO ligand amounts to a length of Ge1–O1 = 1.820(1) Å. This distance is in between the values for the Ge–O distances involving the perfluoropinacol ligands, which show longer bonds for the axial positions (1.836(1) Å,

1.854(1) Å) and shorter bonds for the equatorial positions (1.801(1) Å, 1.802(1) Å). Notably, the S1–O1 distance of 1.596(1) Å is elongated relative to the respective bond lengths in Greb’s octahedral coordinate (cat^{Cl})₂Ge·(Me₂SO)₂ (Ge–O_{DMSO} = 1.561(1) Å, symmetry equivalent).^{6b} Interestingly, Greb’s SC-XRD study also involves an uncoordinated lattice DMSO with a shorter S–O bond length of 1.502(1) Å that may serve as a reference for “free” Me₂SO in the condensed phase. These data indicate that the S=O bond strength in **2**–Me₂SO is slightly lower than in (cat^{Cl})₂Ge·(Me₂SO)₂. We assume that the six-coordinate Ge center in Greb’s compound bearing two Me₂SO donor ligands draws less electron density from each sulfoxide than the five-coordinate Ge center in **2**–Me₂SO, which bears only one Me₂SO donor ligand to compensate its electron deficiency. Future studies might investigate into a correlation between the S–O distance in sulfoxide adducts of potent Lewis acids and their catalytic activity in sulfoxide reduction.

To test the relative affinity of the DMSO ligand to **2**, we added DMF (2 eq.) to a CD₃CN solution of **2**–Me₂SO in an NMR sample tube, and ¹H NMR analysis revealed a marked upfield shift of the CH₃ signal of the DMSO protons. Notably, only one signal (set) for the DMSO (2.83 ppm), as well as the DMF (8.03, 3.00, 2.87 ppm) was observed neither of which corresponded to the respective ¹H chemical shift of the “free” sulfoxide or amide, respectively ($\delta^{(1)\text{H}} = 2.50$ or 7.92, 2.89, and 2.77 ppm in CD₃CN),³³ but was consistently shifted to lower field. This suggests that DMSO and DMF are in a dynamic competitive equilibrium toward coordination to the Ge center in **2** (participation of CD₃CN cannot be fully excluded), which is quick on the NMR timescale (at RT). The addition of Bu₃PO (1.1 eq.) to this mixture resulted in a (further) upfield shift of the DMSO and DMF signals in the ¹H NMR spectrum to values that match the “free” oxo compounds. In the ³¹P{¹H} NMR analysis, one broad resonance at 87.2 ppm was found, which refers to the ³¹P signal observed, as also, upon mixing **2**–MeCN and this phosphine oxide in CD₃CN (without DMSO and DMF). We presume that Bu₃PO majorly extrudes both DMSO and DMF from the Ge complex to furnish the more stable **2**–Bu₃PO. In addition, we converted **2**–Me₂SO with PhSiH₃ (1.5 eq.) in CD₃CN, which resulted in the anticipated formation of Me₂S but also complete decomposition of **2** (and not refurbishing of **2**–Do, Do = SME₂, CD₃CN and Me₂SO, as expected from a “true” catalyst) as concluded from ¹H and ¹⁹F NMR analysis (full conversion after 9 h at 70 °C). This also shows that the Lewis acid-catalyzed reduction of DMSO to DMS with PhSiH₃ can be conducted in MeCN, though conversion rates might be lower.

Considerations in the catalysis mechanism

We have shown using NMR spectroscopy and SC-XRD study that **1** and **2** form strong coordination compounds with Bu₃PO, Me₂SO, and Me₂NCHO. Complex **2**–MeCN was reported to react with hydrosilane to the germylene species **3** and silylated perfluoropinacol and we showed that the latter exhibits weaker catalytic activity.⁸ In contrast, we found **1**–MeCN not to react with PhSiH₃ at RT (¹H, ¹⁹F NMR monitored for 4 h in CD₃CN; at 70 °C traces of new species noted after 2 h). Tilley



proposed a Lewis acid catalysis mechanism for the reduction of aldehydes with Et_3SiH using bis(perfluorocatecholato)silane as catalyst.^{3a} The catalytic cycle marks the initial interaction of the Lewis acid with the carbonyl group of the substrate. An alternative mechanism, which comprises an initial interaction between the Lewis acid and the hydrosilane (to effect weakening of the Si-H bond), was suggested by Oestreich and Stephan for the phosphine oxide reduction with silanes promoted by $\text{B}(\text{C}_6\text{F}_5)_3$ or electrophilic phosphonium cations.^{15a} We reason that for the stronger adducts **1**·Do (Do = R_3PO , Me_2SO , and Me_2NCHO) the direct interaction of the Si center with an SiH group will be even more diminished than for **1**·MeCN. Accordingly, we conclude that the catalytic reductions of the E=O double bonds (E = P, S, C) presented in this study proceed similar to Tilley's Lewis acid catalysis mechanism when **1**·MeCN is used as the promoter. For **2**·MeCN, the situation is more ambiguous due to its pronounced hydride affinity. Consistent to Tilley's mechanism we suggest that the respective complexes **1**·Do or **2**·Do (Do = R_3PO , Me_2SO , Me_2NCHO) mark the actual catalysts which renders the MeCN adducts to assume the role of precatalysts. It is remarkable that **1**·MeCN seems to outperform the more Lewis acidic **B** in catalytic reduction of Ph_3PO (Fig. 1, 2, and Table 1). Notably, strong Lewis acids of perhalogenated bis(catecholato) tetrelanes form hexacoordinate complexes with many Lewis bases, and, in stark contrast, the many bis(perfluoropinacol) tetrelanes which we have structurally characterized, so far, are limited to five-fold coordination. This demonstrates the pronounced impact of the ligand system (catecholate *vs.* pincacolate) on catalyst activity.

Experimental

The relevant experimental work was conducted under an argon atmosphere using standard Schlenk techniques and a glovebox equipment. A general and representative procedure for the phosphine oxide reduction is as follows: an NMR sample tube was charged with the catalyst, and the phosphine oxide and the solids were dissolved in *o*-DFB. The reducing agent was added, and the reaction mixture was heated to the respective temperature for 16 hours. Tris(2,4-di-*tert*-butylphenyl) phosphite was added as an internal standard to determine the yield *via* intensity ratios in the $^{31}\text{P}\{^1\text{H}\}$ NMR spectrum. More detailed experimental data are given in the SI of this article.

Conclusions

The main group Lewis acids **1**·MeCN and **2**·MeCN were successfully applied as precatalysts in the reduction of phosphine oxides (*e.g.* Me_3PO , Bu_3PO , and Ph_3PO), a sulfoxide (*i.e.* Me_2SO), and an amide (*i.e.* Me_2NCHO) to afford the respective phosphines, dimethyl sulfide, and trimethylamine using PhSiH_3 or $(\text{EtO})_3\text{SiH}$. These substrates mark generally more stable element oxygen double bonds in comparison with, for

example, the C=O double bonds in ketones or aldehydes often targeted for demonstrating the catalytic activity of Lewis acids. As benchmarks, we also studied $\text{B}(\text{C}_6\text{F}_5)_3$ and HNTf_2 as reference (soft) Lewis superacid and Brønsted superacid, respectively. Among all the investigated combinations of (pre)catalyst, substrate, and reducing agent, we pronounce the silicon complex **1**·MeCN as the most versatile system, being the by far most potent (DMSO) or just slightly underperforming (R_3PO , DMF) promoter. For the methylated substrates, we sort the ease of catalytic reduction using **1**·MeCN and PhSiH_3 in the order $\text{Me}_2\text{SO} > \text{Me}_3\text{PO} > \text{Me}_2\text{NCHO}$ (most facile to most difficult). Moreover, the hitherto undescribed Lewis acid base adducts **1**· Me_2NCHO and **2**· Me_2SO were synthesized, isolated, and structurally investigated using multinuclear NMR spectroscopy and single-crystal XRD analysis. After probing the reactivity of **1**·MeCN, **2**·MeCN, and **2**· Me_2SO with DMF, DMSO, phosphine oxide, and PhSiH_3 , we conclude that a Lewis acid catalysis mechanism prevails as had been proposed by Tilley for silane Lewis acids. The MeCN complexes act as precatalysts to *in situ* form the catalytically active species **1**·Do or **2**·Do (Do = Me_3PO , Me_2SO , Me_2NCHO). Future studies should focus on extending the scope of sulfoxides and amides, as well as suitable reducing agents. Other substrates such as esters should be investigated, and the water tolerance of the system needs to be examined.

Author contributions

S. I. conceived and guided the study. D. F. and T. F. conceived and conducted the specific experiments. S. S. collected, solved, and refined the SC-XRD data. All authors have co-written the manuscript.

Conflicts of interest

The authors declare no conflict of interest.

Data availability

Supporting data for this article have been included as part of the supplementary information (SI). Supplementary information: detailed experimental and crystallographic data. See DOI: <https://doi.org/10.1039/d5qi02493e>.

Further raw data are available upon reasonable request from the corresponding author.

CCDC 2492264 and 2492265 contain the supplementary crystallographic data for this paper.^{35a,b}

Acknowledgements

The authors are grateful to the European Research Council (ALLOWE101001591) for financial support and thank Tobias Weng for LIFDI-MS analysis.



References

1 (a) D. W. Stephan, Diverse Uses of the Reaction of Frustrated Lewis Pair (FLP) with Hydrogen, *J. Am. Chem. Soc.*, 2021, **143**, 20002–20014; (b) P. P. Power, An Update on Multiple Bonding between Heavier Main Group Elements: The Importance of Pauli Repulsion, Charge-Shift Character, and London Dispersion Force Effects, *Organometallics*, 2020, **39**, 4127–4138; (c) P. P. Power, Main-group elements as transition metals, *Nature*, 2010, **463**, 171–177; (d) G. C. Welch, R. R. S. Juan, J. D. Masuda and D. W. Stephan, Reversible, Metal-Free Hydrogen Activation, *Science*, 2006, **314**, 1124–1126.

2 (a) H. F. T. Klare, L. Albers, L. Sürse, S. Keess, T. Müller and M. Oestreich, Silylium Ions: From Elusive Reactive Intermediates to Potent Catalysts, *Chem. Rev.*, 2021, **121**, 5889–5985; (b) J. B. Lambert, S. Zhang, C. L. Stern and J. C. Huffman, Crystal Structure of a Silyl Cation with No Coordination to Anion and Distant Coordination to Solvent, *Science*, 1993, **260**, 1917–1918.

3 (a) A. L. Liberman-Martin, R. G. Bergman and T. D. Tilley, Lewis Acidity of Bis(perfluorocatecholato)silane: Aldehyde Hydrosilylation Catalyzed by a Neutral Silicon Compound, *J. Am. Chem. Soc.*, 2015, **137**, 5328–5331; (b) L. Greb, Lewis Superacids: Classifications, Candidates, and Applications, *Chem. – Eur. J.*, 2018, **24**, 17881–17896; (c) P. Erdmann and L. Greb, Multidimensional Lewis Acidity: A Consistent Data Set of Chloride, Hydride, Methide, Water and Ammonia Affinities for 183 p-Block Element Lewis Acids, *ChemPhysChem*, 2021, **22**, 935–943; (d) A. Hermannsdorfer and M. Driess, Silicon Tetrakis(trifluoromethanesulfonate): A Simple Neutral Silane Acting as a Soft and Hard Lewis Superacid, *Angew. Chem., Int. Ed.*, 2021, **60**, 13656–13660; (e) A. Y. Timoshkin, The Field of Main Group Lewis Acids and Lewis Superacids: Important Basics and Recent Developments, *Chem. – Eur. J.*, 2024, **30**, e202302457; (f) F. Hanusch, D. Franz and S. Inoue, Uncharged Lewis superacidic silicon complexes—perfluoropinacolato-stabilized systems for homogenous catalysis, *Chem. Lett.*, 2024, **53**, upaea232.

4 A. Hermannsdorfer and M. Driess, Isolable Silicon-Based Polycations with Lewis Superacidity, *Angew. Chem., Int. Ed.*, 2020, **59**, 23132–23136.

5 L. O. Müller, D. Himmel, J. Stauffer, G. Steinfeld, J. Slattery, G. Santiso-Quiñones, V. Brecht and I. Krossing, Simple Access to the Non-Oxidizing Lewis Superacid $\text{PhF}\rightarrow\text{Al}(\text{ORF})_3$ ($\text{RF}=\text{C}(\text{CF}_3)_3$), *Angew. Chem., Int. Ed.*, 2008, **47**, 7659–7663.

6 (a) R. Maskey, M. Schädler, C. Legler and L. Greb, Bis(perchlorocatecholato)silane—A Neutral Silicon Lewis Super Acid, *Angew. Chem., Int. Ed.*, 2018, **57**, 1717–1720; (b) D. Roth, H. Wadeohl and L. Greb, Bis(perchlorocatecholato)germane: Hard and Soft Lewis Superacid with Unlimited Water Stability, *Angew. Chem., Int. Ed.*, 2020, **59**, 20930–20934; (c) T. Thorwart, D. Roth and L. Greb, Bis(pertrifluoromethylcatecholato)silane: Extreme Lewis Acidity Broadens the Catalytic Portfolio of Silicon, *Chem. – Eur. J.*, 2021, **27**, 10422–10427; (d) T. Thorwart, D. Hartmann and L. Greb, Dihydrogen Activation with a Neutral, Intermolecular Silicon(IV)-Amine Frustrated Lewis Pair, *Chem. – Eur. J.*, 2022, **28**, e202202273.

7 F. S. Tschernuth, T. Thorwart, L. Greb, F. Hanusch and S. Inoue, Bis(perfluoropinacolato)silane: A Neutral Silane Lewis Superacid Activates Si–F Bonds, *Angew. Chem., Int. Ed.*, 2021, **60**, 25799–25803.

8 F. S. Tschernuth, A. Kostenko, S. Stigler, A. Gradenegger and S. Inoue, A neutral germanium-centred hard and soft Lewis superacid and its unique reactivity towards hydro-silanes, *Dalton Trans.*, 2024, **53**, 74–81.

9 (a) F. S. Tschernuth, L. Bichlmaier, S. Stigler and S. Inoue, Tuning the Lewis Acidity of Neutral Silanes Using Perfluorinated Aryl- and Alkoxy Substituents, *Eur. J. Inorg. Chem.*, 2023, **26**, e202300388; (b) F. S. Tschernuth, L. Bichlmaier and S. Inoue, Catalytic Degradation of Aliphatic Ethers using the Lewis Superacidic Bis(perfluoropinacolato)silane, *ChemCatChem*, 2023, **15**, e202300281.

10 (a) P. A. Byrne and D. G. Gilheany, The modern interpretation of the Wittig reaction mechanism, *Chem. Soc. Rev.*, 2013, **42**, 6670–6696; (b) B. E. Maryanoff and A. B. Reitz, The Wittig olefination reaction and modifications involving phosphoryl-stabilized carbanions. Stereochemistry, mechanism, and selected synthetic aspects, *Chem. Rev.*, 1989, **89**, 863–927; (c) K. C. K. Swamy, N. N. B. Kumar, E. Balaraman and K. V. P. P. Kumar, Mitsunobu and Related Reactions: Advances and Applications, *Chem. Rev.*, 2009, **109**, 2551–2651; (d) S. Fletcher, The Mitsunobu reaction in the 21st century, *Org. Chem. Front.*, 2015, **2**, 739–752.

11 T. Coumbe, N. J. Lawrence and F. Muhammad, Titanium (IV) catalysis in the reduction of phosphine oxides, *Tetrahedron Lett.*, 1994, **35**, 625–628.

12 Y. Li, S. Das, S. Zhou, K. Junge and M. Beller, General and Selective Copper-Catalyzed Reduction of Tertiary and Secondary Phosphine Oxides: Convenient Synthesis of Phosphines, *J. Am. Chem. Soc.*, 2012, **134**, 9727–9732.

13 (a) H. Fritzsche, U. Hasserodt and F. Korte, Reduktion organischer Verbindungen des fünfwertigen Phosphors zu Phosphinen, I. Reduktion tertiärer Phosphinoxyde zu tertiären Phosphinen mit Silanen, *Chem. Ber.*, 1964, **97**, 1988–1993; (b) L. Horner and W. D. Balzer, Phosphororganische Verbindungen IXL zum sterischen Verlauf der Desoxygierung von tertiären phosphinoxyden zu tertiären phosphinen mit trichlorsilan, *Tetrahedron Lett.*, 1965, **6**, 1157–1162; (c) K. Naumann, G. Zon and K. Mislow, Use of hexachlorodisilane as a reducing agent. Stereospecific deoxygenation of acyclic phosphine oxides, *J. Am. Chem. Soc.*, 1969, **91**, 7012–7023.

14 (a) D. Héault, D. H. Nguyen, D. Nuel and G. Buono, Reduction of secondary and tertiary phosphine oxides to phosphines, *Chem. Soc. Rev.*, 2015, **44**, 2508–2528; (b) E. Podyacheva, E. Kuchuk and D. Chusov, Reduction of phosphine oxides to phosphines, *Tetrahedron Lett.*, 2019, **60**, 575–582.



15 (a) M. Mehta, I. Garcia de la Arada, M. Perez, D. Porwal, M. Oestreich and D. W. Stephan, Metal-Free Phosphine Oxide Reductions Catalyzed by B(C₆F₅)₃ and Electrophilic Fluorophosphonium Cations, *Organometallics*, 2016, **35**, 1030–1035; (b) A. Chardon, O. Maubert, J. Rouden and J. Blanchet, Metal-Free Reduction of Phosphine Oxides, Sulfoxides, and N-Oxides with Hydrosilanes using a Borinic Acid Precatalyst, *ChemCatChem*, 2017, **9**, 4460–4464.

16 P. Erdmann and L. Greb, What Distinguishes the Strength and the Effect of a Lewis Acid: Analysis of the Gutmann–Beckett Method, *Angew. Chem., Int. Ed.*, 2022, **61**, e202114550.

17 (a) O. M. Demchuk, R. Jasiński and K. M. Pietrusiewicz, New Insights into the Mechanism of Reduction of Tertiary Phosphine Oxides by Means of Phenylsilane, *Heteroat. Chem.*, 2015, **26**, 441–448; (b) K. L. Marsi, Phenylsilane reduction of phosphine oxides with complete stereospecificity, *J. Org. Chem.*, 1974, **39**, 265–267.

18 (a) Y. Takahashi, T. Mitsudome, T. Mizugaki, K. Jitsukawa and K. Kaneda, Highly Efficient Deoxygenation of Sulfoxides Using Hydroxyapatite-supported Ruthenium Nanoparticles, *Chem. Lett.*, 2014, **43**, 420–422; (b) D. L. Lourenço and A. C. Fernandes, Reduction of sulfoxides catalyzed by the commercially available manganese complex MnBr(CO)5, *Org. Biomol. Chem.*, 2024, **22**, 3746–3751; (c) S. Enthaler and M. Weidauer, Reduction of Sulfoxides to Sulfides in the Presence of Copper Catalysts, *Catal. Lett.*, 2011, **141**, 833–838.

19 D. Porwal and M. Oestreich, B(C₆F₅)₃-Catalyzed Reduction of Sulfoxides and Sulfones to Sulfides with Hydrosilanes, *Synthesis*, 2017, 4698–4702.

20 (a) C. Edinger and S. R. Waldvogel, Electrochemical Deoxygenation of Aromatic Amides and Sulfoxides, *Eur. J. Org. Chem.*, 2014, 5144–5148; (b) Z. Kong, C. Pan, M. Li, L. Wen and W. Guo, Scalable electrochemical reduction of sulfoxides to sulfides, *Green Chem.*, 2021, **23**, 2773–2777.

21 J. Zhao, Z. Luo, Y. Liu, S. Chen, J. He, J. Xu, W. Hu, Z. Huang and W. Xiong, Visible light induced deoxygenation of sulfoxides with isopropanol, *Org. Chem. Front.*, 2023, **10**, 5254–5259.

22 (a) M. Madesclaire, Reduction of sulfoxides to thioethers, *Tetrahedron*, 1988, **44**, 6537–6580; (b) F. Takahashi, K. Nogi and H. Yorimitsu, B2cat2-Mediated Reduction of Sulfoxides to Sulfides, *Eur. J. Org. Chem.*, 2020, 3009–3012.

23 H. Schindelin, C. Kisker, J. Hilton, K. V. Rajagopalan and D. C. Rees, Crystal Structure of DMSO Reductase: Redox-Linked Changes in Molybdopterin Coordination, *Science*, 1996, **272**, 1615–1621.

24 B. R. James, F. T. T. Ng and G. L. Rempel, Catalytic reduction of dimethylsulfoxide by molecular hydrogen using rhodium(III) complexes, *Can. J. Chem.*, 1969, **47**, 4521–4526.

25 R. Simó, J. O. Grimalt and J. Albaigés, Sequential Method for the Field Determination of Nanomolar Concentrations of Dimethyl Sulfoxide in Natural Waters, *Anal. Chem.*, 1996, **68**, 1493–1498.

26 B. J. Anness and C. W. Bamforth, DIMETHYL SULPHIDE—A REVIEW, *J. Inst. Brew.*, 1982, **88**, 244–252.

27 (a) S. Kronig, E. Theuerberg, D. Holschumacher, T. Bannenberg, C. G. Daniliuc, P. G. Jones and M. Tamm, Dihydrogen Activation by Frustrated Carbene-Borane Lewis Pairs: An Experimental and Theoretical Study of Carbene Variation, *Inorg. Chem.*, 2011, **50**, 7344–7359; (b) J.-M. Denis, H. Forintos, H. Szelke, L. Toupet, T.-N. Pham, P.-J. Madec and A.-C. Gaumont, B(C₆F₅)₃-catalyzed formation of B–P bonds by dehydrocoupling of phosphine-boranes, *Chem. Commun.*, 2003, 54–55.

28 (a) D. W. Stephan, Frustrated Lewis Pairs: From Concept to Catalysis, *Acc. Chem. Res.*, 2015, **48**, 306–316; (b) A. Berkefeld, W. E. Piers and M. Parvez, Tandem Frustrated Lewis Pair/Tris(pentafluorophenyl)borane-Catalyzed Deoxygenative Hydrosilylation of Carbon Dioxide, *J. Am. Chem. Soc.*, 2010, **132**, 10660–10661.

29 Y. E. Jad, G. A. Acosta, S. N. Khattab, B. G. de la Torre, T. Govender, H. G. Kruger, A. El-Faham and F. Albericio, Peptide synthesis beyond DMF: THF and ACN as excellent and friendlier alternatives, *Org. Biomol. Chem.*, 2015, **13**, 2393–2398.

30 (a) H. Liu, M.-J. Li, X.-N. Zhang, S. Wang, L.-X. Li, F.-F. Guo and T. Zeng, N,N-dimethylformamide-induced acute liver damage is driven by the activation of NLRP3 inflammasome in liver macrophages of mice, *Ecotoxicol. Environ. Saf.*, 2022, **238**, 113609; (b) Y. Lei, S. Xiao, S. Chen, H. Zhang, H. Li and Y. Lu, N,N-dimethylformamide-induced acute hepatic failure: A case report and literature review, *Exp. Ther. Med.*, 2017, **14**, 5659–5663.

31 (a) V. P. Taori and M. R. Buchmeiser, Tandem-reduction of DMF with silanes via necklace-type transition over Pt(0) nanoparticles: deciphering the dual Si–H effect as an extension of steric effects, *Chem. Commun.*, 2014, **50**, 14820–14823; (b) J. L. Martinez, H. K. Sharma, R. Arias-Ugarte and K. H. Pannell, Platinum-Catalyzed Reduction of DMF by 1,1,3,3-Tetramethyldisiloxane, HMeSi₂OSiMe₂H: New Intermediates HSiMe₂OSiMe₂OCH₂NMe₂ and HSiMe₂(OSiMe₂)₃OCH₂NMe₂ and Their Further Chemical Reactivity, *Organometallics*, 2014, **33**, 2964–2967; (c) R. Arias-Ugarte, H. K. Sharma, A. L. C. Morris and K. H. Pannell, Metal-Catalyzed Reduction of HCONR'2, R' = Me (DMF), Et (DEF), by Silanes to Produce R'2NMe and Disiloxanes: A Mechanism Unraveled, *J. Am. Chem. Soc.*, 2012, **134**, 848–851; (d) H. K. Sharma, R. Arias-Ugarte, D. Tomlinson, R. Gappa, A. J. Metta-Magaña, H. Ito and K. H. Pannell, (Me₃N)Mo(CO)₅-Catalyzed Reduction of DMF by Disiloxane and Disilane Moieties: Fate of the Silicon-Containing Fragments, *Organometallics*, 2013, **32**, 3788–3794.

32 (a) Y. Li and C. Cui, Cesium Carbonate-Catalyzed Oxidation of Substituted Phenylsilanes for the Efficient Synthesis of Polyhedral Oligomeric Silsesquioxanes, *Inorg. Chem.*, 2018, **57**, 13477–13485; (b) W. Xie, M. Zhao and C. Cui, Cesium Carbonate-Catalyzed Reduction of Amides with Hydrosilanes, *Organometallics*, 2013, **32**, 7440–7444.



33 G. R. Fulmer, A. J. M. Miller, N. H. Sherden, H. E. Gottlieb, A. Nudelman, B. M. Stoltz, J. E. Bercaw and K. I. Goldberg, NMR Chemical Shifts of Trace Impurities: Common Laboratory Solvents, Organics, and Gases in Deuterated Solvents Relevant to the Organometallic Chemist, *Organometallics*, 2010, **29**, 2176–2179.

34 H. Borrman, I. Persson, M. Sandström and C. M. V. Stålhandske, The crystal and liquid structures of N,N-dimethylthioformamide and N,N-dimethylformamide showing a stronger hydrogen bonding effect for C–H···S than of C–H···O, *J. Chem. Soc., Perkin Trans. 2*, 2000, 393–402.

35 (a) CCDC 2492264: Experimental Crystal Structure Determination, 2026, DOI: [10.5517/ccdc.csd.cc2pndmd](https://doi.org/10.5517/ccdc.csd.cc2pndmd); (b) CCDC 2492265: Experimental Crystal Structure Determination, 2026, DOI: [10.5517/ccdc.csd.cc2pndnf](https://doi.org/10.5517/ccdc.csd.cc2pndnf).

